Pulsed Plasma Actuators for Active Flow Control at MAV Reynolds Numbers

B. Göksel[1], D. Greenblatt[2], I. Rechenberg[1], Y. Kastantin[2]
C.N. Nayeri[2], C.O. Paschereit[2]
[1]Email: info@electrofluidsystems.com
[1]Technical University Berlin, Institute of Process Engineering
Ackerstr. 71-76, Secr. ACK1, D-13355 Berlin, Germany
[2] Technical University Berlin, Hermann-Föttinger-Institute of Fluid Mechanics
Müller-Breslau-Strasse 8, D-10623 Berlin, Germany

Summary

An experimental investigation of separation control using steady and pulsed plasma actuators was carried out on an Eppler E338 airfoil at typical micro air vehicle Reynolds numbers ($20,000 \leq Re \leq 140,000$). Pulsing was achieved by modulating the high frequency plasma excitation voltage. The actuators were calibrated directly using a laser doppler anemometer, with and without free-stream velocity, and this allowed the quantification of both steady and unsteady momentum introduced into the flow. At conventional low Reynolds numbers ($Re>100,000$) asymmetric single phase plasma actuators can have a detrimental effect on airfoil performance due to the introduction of low momentum fluid into the boundary layer. The effect of modulation, particularly at frequencies corresponding to $F^+ \approx 1$, became more effective with decreasing Reynolds number resulting in significant improvements in $C_{L,\max}$. This was attributed to the increasing momentum coefficient, which increased as a consequence of the decreasing free-stream velocities. Particularly low duty cycles of 3% were sufficient for effective separation control, corresponding to power inputs on the order of 5 milliwatts per centimeter.

1 Introduction

Achieving sustained flight of micro air vehicles (MAVs) bring significant challenges due to their small dimensions and low flight speeds. This combination results in very low flight Reynolds numbers ($Re<200,000$), where conventional low-Reynolds-number airfoils perform poorly, or even generate no useful lift. Some of the best performing airfoils in this Re range are cambered flat plates and airfoils with a thickness to chord ratio (t/c) of approximately 5% [1], [2]. MAV are usually designed with surveillance, sensing or detection in mind. Hence, a typical MAV mission should include a "high speed dash" (V~65km/h, 18m/s) to or from a desired location with significant head or tail winds, and low-speed loiter (V~30km/h, 8.3m/s) while maneuvering, descending and climbing [3]. Mueller defines two MAV sizes, which we can call "large" (b=15cm, M=90g) and "small" (b=8cm, M=30g) [1].

The generation of useful lift at $Re<50,000$ is particularly challenging because passive tripping of the boundary layer is virtually impossible [5]. Consequently, unconventional approaches have been pursued, such as ornithopters that are inspired by bird and insect flight. Active control methods are also pursued. For example, Greenblatt & Wygnanski investigated perturbing an airfoil leading-edge boundary layer via two-dimensional periodic excitation at $Re=50,000$ and $30,000$ [8]. Near-sinusoidal pertubations at $F^+\approx1$ resulted in the restoration of conventional low-Reynolds-number lift and aerodynamic efficiency, while excitation-induced lift oscillations were small and hysteresis associated with stall was eliminated. However, with decreasing Re larger periodic perturbations (expresses as $\langle C_\mu \rangle$) were required to generate useful lift. A similarity between the timescales associated with excitation and those characterizing dynamic stall in small flying creatures provided some insight into these observations. They observed that typical MAV dimensions are suited to actuation by means of micro-electromechanical systems (MEMS)-based devices. It was also noted that the effectiveness and efficiency of actuators required to supply the prescribed excitation will ultimately determine the success and limitations of the method.

## 2   Motivation for the Present Study

To illustrate the challenges facing development of these vehicles, let us define the wing aspect ratio: $AR = b/\bar{c}$ where $\bar{c}$ is the standard mean chord and assume that for typical MAVs: $1 \le AR \le 2$. Furthermore, we define a characteristic Reynolds number $Re = V\bar{c}/\nu$ and lift coefficient:

$$C_L = L / \tfrac{1}{2}\rho V^2 A \ . \tag{1}$$

Using the definitions of aspect ratio and lift coefficient above and assuming straight and level flight, we can express the stall speed as follows:

$$V_{\text{stall}} = \sqrt{\frac{2Mg / AR}{\rho b^2 C_{L,\max}}} \ . \tag{2}$$

Now, using definitions of "small" and "large" MAVs defined above, we generate V_{stall} versus C_L curves corresponding to $AR=1$ and 2, Figure 1. Also shown are the target loiter speed and corresponding Reynolds numbers. It is evident that the smaller vehicle requires a larger $C_{L,\max}$ with simultaneously lower Reynolds number at the loiter target. Furthermore, wings with $AR>1$ are required to produce significantly larger $C_{L,\max}$ at lower Reynolds number. Conventional low Reynolds number UAVs, where typically $Re>200,000$, achieve loiter targets by deploying flaps. This is not considered practical for MAVs loitering at $Re<50,000$, where passive tripping of the boundary layer in order to generate useful lift is not possible.
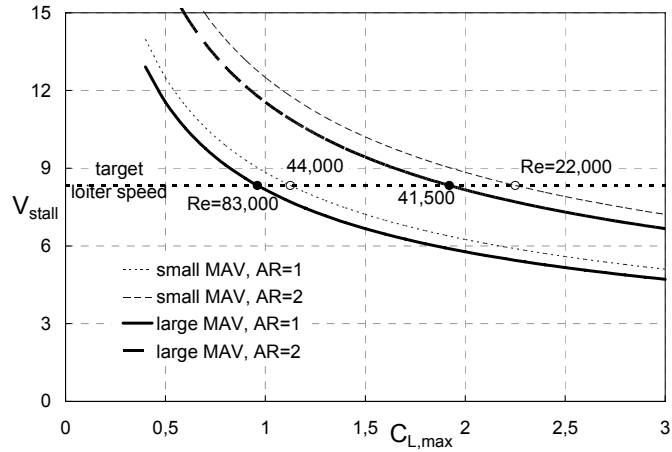
Figure 1 Stall speed as a function of maximum lift coefficient for "small" and "large" (see definitions in section 1) MAVs at two different aspect ratios.

Figure 2 shows airfoil section $C_{L,\mathrm{max}}$ for conventional low Reynolds number air-foils and reflects the well-known performance deterioration with reducing *Re*. Thus the problem of attaining low loiter speeds is compounded because perform-ance degradation due to lower Reynolds number conflicts with higher $C_{L,\mathrm{max}}$ requirements. It is emphasized that loiter is a mission critical flight regime, where the MAV performs its primary function such as surveillance or sensing.
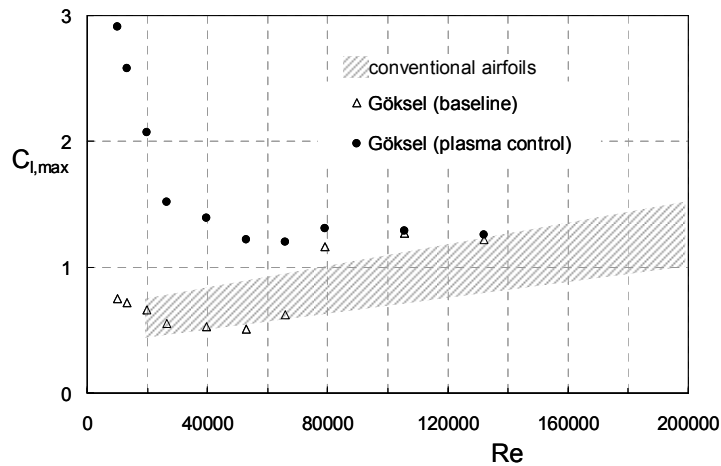
Figure 2 Graph showing the baseline and plasma control data together with performance degradation of conventional low airfoils with reducing Reynolds number [9]. Power sup-plied to the corona discharge wires is approximately 8.5Watts.

Plasma-based actuators have recently demonstrated application to separation control [9], [10], [11], [13], [14], [15]. The first separation flow control on airfoils at typical MAV Reynolds numbers (13,000<Re<140,000) were demonstrated by plasma actuation using high voltage (10–20 kV) charged corona discharge wires in 1999 [9], [10]. Göksel demonstrated significant improvement to an Eppler E338 airfoil performance [e.g. $C_{L,\max}$, $(l/d)_{\max}$], particularly for 10,000<Re<70,000 [9].

For a given power input (in this case ~8.5Watts) $C_{L,\max}$ was shown to increase with decreasing Reynolds number up to 2.9 at Re=10,000. The reason for this is that the relative power input by the actuators increased with decreasing Re.

To illustrate this, we define the two-dimensional power coefficient:

$$C_W = W / \tfrac{1}{2}\rho U_\infty^3 c , \qquad (3)$$

and note that for the data presented in Figure 2, W remains constant and thus $C_W \propto 1/U_\infty^3$. A similar argument is assumed to apply to the steady two-dimensional momentum coefficient

$$C_\mu = J / \tfrac{1}{2}\rho U_\infty^2 c , \qquad (4)$$

where the steady wall-jet momentum produced immediately downstream of the actuator, namely:

$$J = \int_0^\infty \rho U_J^2 dy \qquad (5)$$

The potential application of plasma actuators to the MAV is clearly evident by comparing Figures 1 and 2. Here it is seen that the requirement for high C_L in the loiter regime can be met by plasma actuation. However, the power requirement was relatively high (~8.5W) corresponding to $C_{W,\max} \leq 137$ for the range of Reynolds numbers considered. Moreover, calibration of the corona wires by measuring downstream mean velocity profiles, indicated that $C_{\mu,\max}$>10%, thereby indicating that at low Reynolds numbers circulation control is possible [17].

Several comparisons of separation control by periodic excitation versus steady blowing have indicated that similar performance benefits (e.g. ΔC_L) can be achieved where $\langle C_\mu \rangle$ is up to two orders of magnitude smaller than C_μ. Using plasma actuators in a pulsed mode, Corke et al. have shown that steady forcing produced negligible changes to $C_{L,\max}$ while unsteady forcing at F^+=1 resulted in $\Delta C_{L,\max} \approx 0.2$ [11]. Performance improvements using pulsed actuation were demonstrated on a delta wing using piezo-electric actuators by Margalit et al. [16].

The present investigation was undertaken to examine the possibility of controlling separation using plasma actuators in a pulsed mode at typical MAV Reynolds numbers. A pulsed plasma jet, generated using the single phase actuation technique near the leading edge of the airfoil (x/c=1%) was utilized for this purpose [15]. Data were compared with both 2D and 3D boundary layer tripping. The momentum added to a flow by means of pulsed actuation introduces both time-mean and unsteady components of momentum. To quantify this, a separated experiment was conducted to calibrate the actuators and hence estimate both steady and unsteady components of momentum (C_μ, $\langle C_\mu \rangle$).

3   The Experiments

3.1   Actuator Calibration Setup

Calibration of the actuator was conducted in a closed-loop wind tunnel with a 2m long test section of 400 x 280mm in a quiescent environment ($U_\infty = 0$) and at free-stream velocities corresponding to the Reynolds numbers tested here. All boundary layers were laminar at the test location. A splitter plate with an elliptical leading edge was installed in the tunnel. The plasma actuator was placed 0.57m downstream of the leading-edge and consisted of two thin metal electrodes separated by a thin dielectric layer, Figure 3 [11], [12], [13]. Sufficiently high voltages (at low radio frequencies in the kHz-range) supplied to the actuator causes the air to weakly ionize at the edges of the upper electrodes. These are regions of high electric field potential. In this asymmetric configuration, the plasma is only generated at one edge, Figure 3. The plasma moves to regions of increasing electric field gradients and induces a 2-D wall jet in the flow direction along the surface, thereby adding momentum to the boundary layer [6].
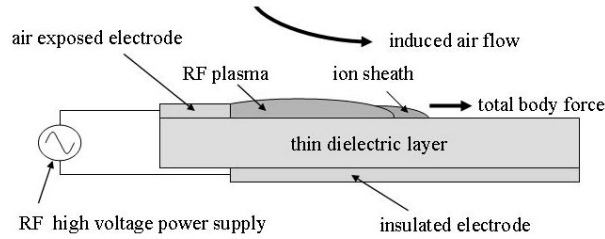
Figure 3   Schematic of the plasma actuator used for the present experiments.

Performing LDV profile measurements, at 3mm, 12mm and 25 mm downstream of the actuator, the steady momentum in the jet was quantified by

$$J = \int_0^\infty \rho(u_J^2 - u^2)dy ,$$ (6)

where u is the time-mean velocity profile without plasma actuation. For the purpose of pulsed (or unsteady) actuation, the wave modulation method was employed where the kHz carrier wave is modulated by a square-wave that correspond to low frequencies appropriate for separation control [11], [14], [15], [16]. This introduces mean (u_J) and unsteady ($\tilde{u}_J$ and $\tilde{v}_J$) velocity components and thus the jet momentum is made up of time-mean and oscillatory component quantified by

$$J_{\text{tot}} = J + \langle J \rangle = \int_0^\infty \rho(u_J^2 - u^2)dy + \int_0^\infty \rho(\tilde{u}_J^2 + \tilde{v}_J^2)dy, \qquad (7)$$

where the first term represents the steady contribution and the second term represents the oscillatory contribution. Consequently, the total momentum coefficient is defined as $C_{\mu,\text{tot}} = C_\mu + \langle C_\mu \rangle$ and also expressed as ($C_\mu, \langle C_\mu \rangle$). For all data acquired here, the actuator was excited with a signal of intermittent bursts of 4.0 kHz that were modulated in the range of 2.5 to 100 Hz. The duty cycle was varied from 1% to 100% at constant voltage.

3.2   Airfoil Setup and Testing

Experiments were performed on an Eppler E338 airfoil (c=17.8cm, b=50cm) mounted between circular endplates downstream of the exit of a 600mm and a 1200mm diameter low speed open jet wind tunnel. Lift and drag were measured using a two component balance. This airfoil was previously used for flow control experiments with high voltage (10–20kV) charged corona discharge wires, and a full description of the setup can be found in [9], [13], [15]. The plasma actuator consisted of two thin metal electrodes separated by a dielectric layer which formed part of the airfoil surface, Figure 3 [11], [12], [13]. Airfoil performance was also assessed by tripping the boundary layer using a three-dimensional (3D) turbulator of height 200 microns and a two-dimensional (2D) step of height 100 microns, at x/c=1%.

## 4   Discussion of Results

4.1   Actuator Calibration

LDV for data for u and $\tilde{u}_J$ at 3mm downstream of the actuator are shown for $U_\infty = 0.83$m/s and $U_\infty = 5.79$m/s in Figures 4a, b and 5a, b respectively. For all data acquired $\tilde{v}_J^2 << \tilde{u}_J^2$ and could consequently be ignored without materially changing the results of equation (7). With no actuation (plasma off), a laminar Blasius boundary layer forms on the plate. At the lower velocity, jet actuation at all duty cycles considered here produces a significant steady and unsteady near wall momentum. In general, larger duty cycles produce larger near-wall mean-flow jets. On the other hand, driving the actuator in burst mode produces larger oscillatory components of momentum, Table 1. Driving the actuator at 100% duty

cycle produces a momentum deficit from approximately 2-3mm from the wall. This is believed to be a consequence of the vortical flow associated with the wall jet, Figure 4a. Also, a mild momentum surplus is generated for all actuator duty cycles in the outer part of the boundary layer. Note that no distinction has been drawn here between purely periodic perturbations and turbulent fluctuations, consequently $\tilde{u}_J$ is representative of the overall unsteadiness u'.

As the free-stream velocity increases the relative momentum added to the flow decreases significantly. At $U_\infty = 5.79$m/s corresponding to Re=70,000, both steady and unsteady components of momentum are negligible, Figures 5a and 5b. Based on these data it is not expected that the plasma actuators will have a significant separation control effect for Re>70,000.
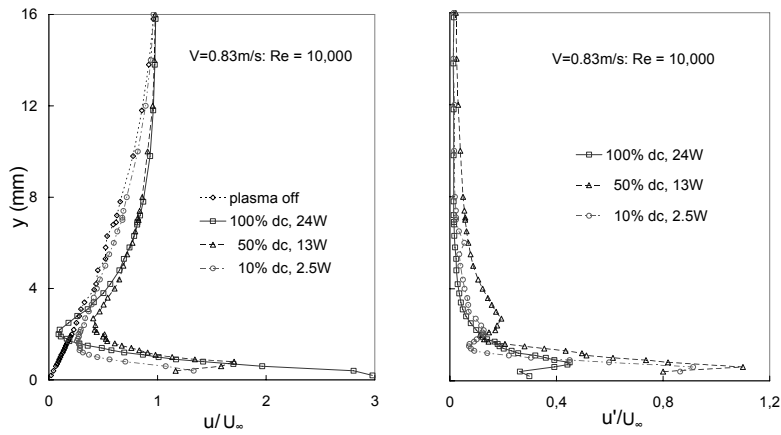
Figure 4 Normalized mean velocity and turbulence intensity at the lowest finite free-stream velocity tested.
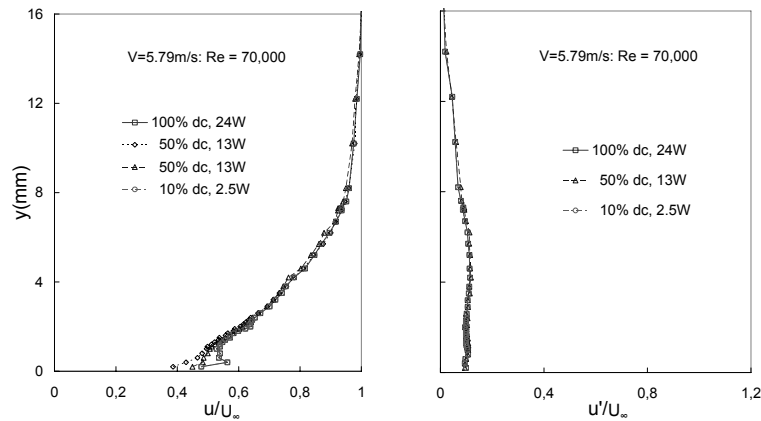
Figure 5 Normalized mean velocity and turbulence intensity at an intermediate free-stream velocity.
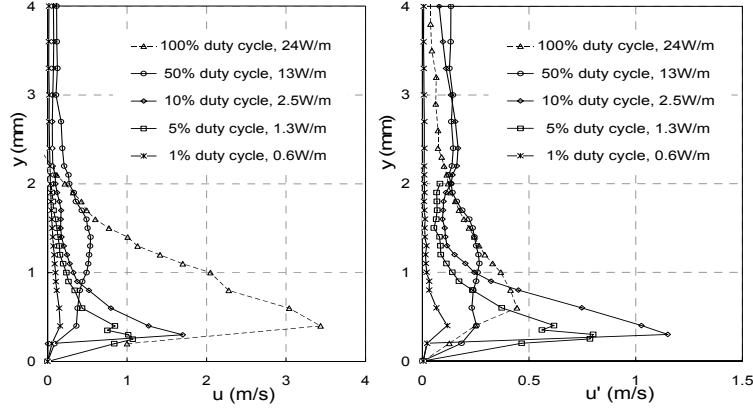
Figure 6 Actuator calibration at 3mm downstream for different duty cycles at $U_\infty = 0$.

Table 1 Steady and unsteady actuator calibrations at various free stream velocities

| Duty Cycle (%)	C_μ (%)	$\langle C_\mu \rangle$ (%)	U_∞ (m/s)
100	8.31	0.25	0.83
50	5.41	0.93	0.83
10	1.76	0.54	0.83
100	1.05	0.025	2.50
50	0.36	0.054	2.50
10	0.018	0.018	2.50
100	0.74	0.009	4.15
50	0.38	0.014	4.15
10	0.02	0.008	4.15

Figure 6 shows actuator calibration data for $U_\infty = 0$. In this case the duty cycle was gradually increased from 1% to 100%. It was noted that a duty cycle threshold between 2% and 4% is reached where there is a significant increase in near-wall unsteady momentum. Peak unsteady momentum is reached at a duty cycle of approximately 10%. Further increases in duty cycle result in decreases to both steady and unsteady near wall momentum. At 100% duty cycle a near-steady wall jet is formed with relatively large mean near wall momentum.

4.2   Airfoil Performance Data

The airfoil data is presented below in terms of deceasing Reynolds number, starting at typical low Re~140,000 (conventional low Re, Figure 7) and reducing to ~20,000 (approximate lower MAV limit). Maximum errors associated with C_L and C_D were ±0.02, and this unfortunately precluded the recording of meaningful C_D measurements at lower Reynolds numbers.

We note that plasma control at 100% duty cycle has a *detrimental* effect and reduces $C_{L,\max}$. This is because a relatively slow speed *steady jet* is being generated by the plasma actuator that is much less than the free-stream velocity with $C_\mu \approx 0.1\%$ (see section 2). Hence, the low momentum fluid introduced near the wall, in fact, promotes separation. This may appear counterintuitive, but a similar effect was noted when using conventional steady slot blowing with $U_J / U_\infty < 1$ [4].
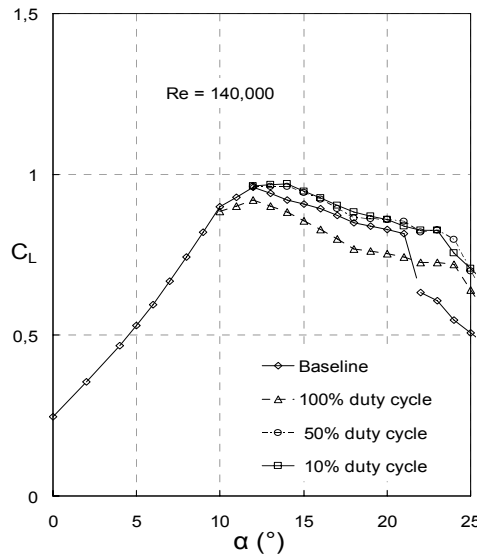
Figure 7 Example of the effect of plasma actuation at $F^+=1$ on airfoil performance at conventional low Reynolds numbers.

All other duty cycles considered ($\leq 50\%$, corresponding to $F^+=1$) have a net positive post-stall effect with relatively low $\langle C_\mu \rangle < 0.1\%$. Changes to post-stall lift and small changes to $C_{L,\max}$ at conventional low Reynolds numbers have been observed by others (e.g. [11], [15]). Interestingly, data is marginally superior when the duty cycle is reduced from 50% to 10%. This might have been expected when considering the data in Figure 6b, which shows that the 10% duty cycle actuation produced greater unsteady near-wall momentum. Moreover, this result is even more significant when we account for the fact that duty cycle percentage correlates linearly with power consumption.

With Reynolds number reduced to 80,000, the near wall jet velocity is comparable to that in the near wall boundary layer and the detrimental effect on $C_{L,\max}$ disappears (not shown). At high post-stall angles, when the airfoil is fully stalled, the jet has a positive effect on C_L (not shown).
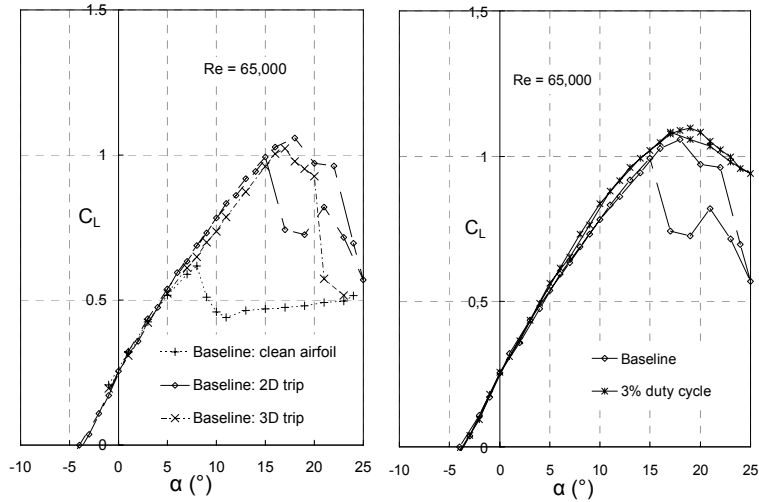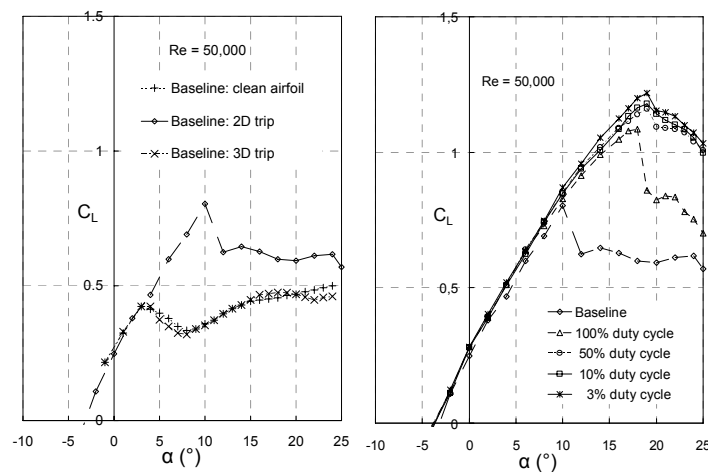
Figure 8 Example of the effect of plasma actuation at F^+=1 on airfoil performance at Reynolds numbers Re=65,000.

At Re=65,000 the baseline clean airfoil performed poorly, but its performance improved with the addition of either 2D or 3D tripping, Figure 8a. 2D tripping was slightly superior, but the airfoil still suffered from significant hysteresis., In contrast, pulsed control at F^+=1 and 3% duty cycle virtually eliminating hysteresis and produced a slight increase in $C_{L,\max}$.

At Re=50,000, also shown here for F^+=1.0, the effect of plasma actuation can be far more clearly observed, Figure 9a,b. As mentioned above [5], and shown in Figure 9a, it is virtually impossible to effectively promote transition passively at these Reynolds numbers, although the 2D trip was more effective than the 3D trip. This is reflected in the poor performance of the airfoil with $C_{L,\max} < 0.8$. For the purposes of presenting an unbiased evaluation, all plasma actuation data presented in the remainder of this paper were compared with that of the 2D trip. In this instance, the 100% duty cycle actuation has a net positive effect on $C_{L,\max}$ and this is because it generates a steady wall jet corresponding to C_μ=0.74%, Table 1.

Successive reductions in duty cycle clearly result in improvements in performance, both with respect to the C_L-α linearity as well as $C_{L,\max}$. Note, in addition, that $C_{L,\max}$ is larger than that at the higher Reynolds numbers. It is assumed that this is due to the larger C_μ values which increase as a consequence of the reducing free-stream velocity. This runs counter to the typical baseline trends and has clear potential for reducing loiter speed discussed in the introduction.

Traditional steady separation is usually characterized by a proportionality between a performance indicator (e.g. $C_{l,\max}$) and C_μ [4], but this is not always the case when control is periodic [7]. For the data present in Figure 5, the conventional arguments of additional unsteady near wall momentum can be applied for duty cycles between 100% and 10% as discussed above. However, performance continues to improve as the duty cycle is reduced from 10% to 3%, Figure 9, despite the decreasing near wall momentum, Figure 6. This is a perplexing phenomenon, but has practical ramifications when it is considered that power supplied to the actuators is proportional to duty cycle.


Figure 9 Example of the effect of plasma actuation at F^+=1 on airfoil performance at Reynolds numbers Re=50,000.

Further reductions in Reynolds number to 35,000 and 20,500 showed ever greater effects on control. For example, in the latter case (Re=20,500) which is very near the low end of the MAV Reynolds number range, significant effect were observed and hence additional data were acquired in an attempt to optimize control. Employing a 5% duty cycle and placing the airfoil at a post stall angle of attack (α = 18°) a frequency scan was performed for the range $0.25 \le F^+ \le 10.4$, Figure 10. The optimum is seen to be at $F^+ \approx 1$ and this is consistent with conventional low Reynolds number data [7]. Corke et al. observed that, using plasma actuators, the minimum voltage required to attach a post-stall separated flow was at $F^+ \approx 1$ [11].

Similar effects have also been observed on delta wings using zero mass-flux jets [16]. Further attempts at optimisation considered variation of the duty cycle. It was observed that the optimum lies somewhere between 3% and 8%. Figure 11. Interestingly, this is the range where the maximum oscillatory momentum is added to the flow.
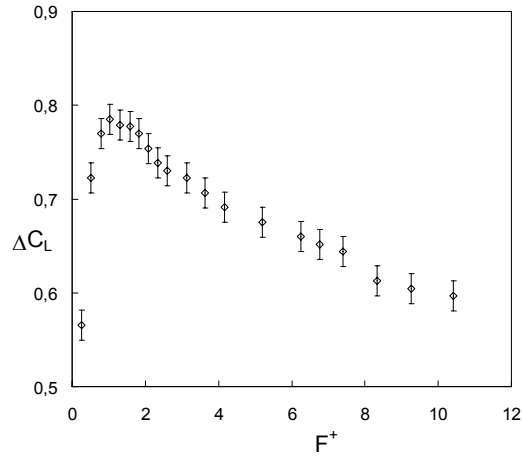
Figure 10 Effect of reduced frequency on post-stall (α=18° airfoil lift at a low MAV Reynolds number; Re=20,500). C_μ=0.05% and duty cycle = 3%.
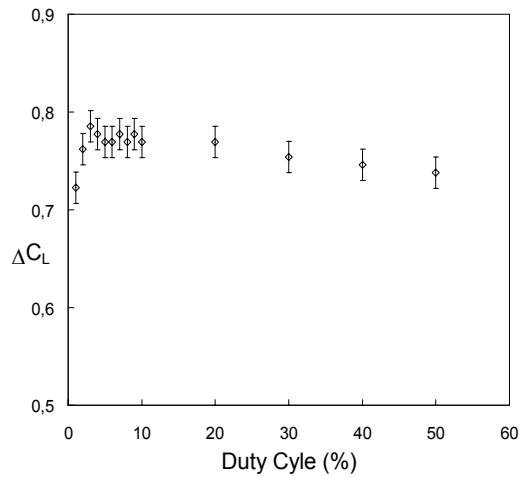

Figure 11 Effect of duty cycle on post-stall (α=18° airfoil lift at a low MAV Reynolds number; Re=20,500).

Finally, the effect of input voltage on the C_L versus α curves was investigated. It was determined that for V>8kVpp (corresponding to 0.5W/m), the effect on the airfoil performance is clearly significant and $C_{L,max}$ is larger than at the higher Reynolds numbers, Figure 12. Note that here the optimum F^+ and duty cycles have been used. Data was generated for increasing α (filled symbols) and decreasing α (open symbols). Note that below 10kVpp the C_L versus α curve is non linear, but this non linear feature does not show any significant hysteresis trend repeats for decreasing α, Figures 12 and 13.
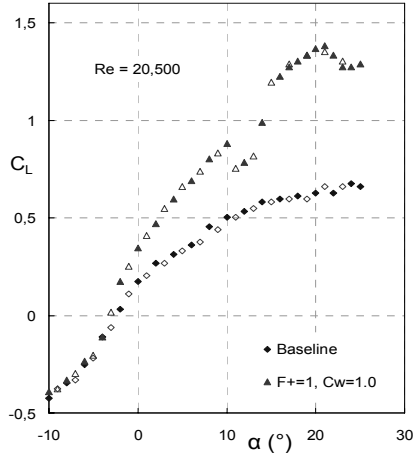
Figure 12 Effect of plasma actuation on airfoil performance at a low MAV Reynolds number illustrating non-linear behavior at low C_W. C_μ=0.04% and duty cycle = 3%.
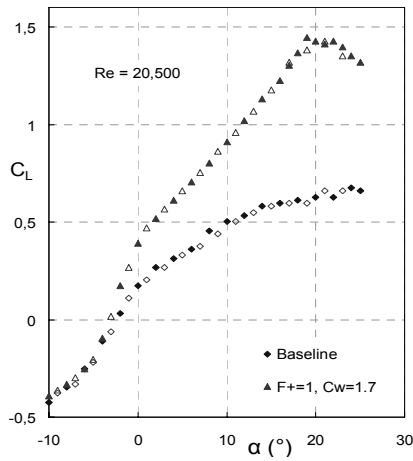
Figure 13 Effect of plasma actuation on airfoil performance at a low MAV Reynolds number illustrating the minimum C_W required for linear behavior. C_μ=0.05% and duty cycle = 3%.

5   Conclusion

The present investigation considered separation control using steady and pulsed plasma actuation on an airfoil at typical MAV Reynolds numbers. Pulsing was achieved by modulating the high frequency plasma excitation voltage. The actuators were calibrated directly and variations of the duty cycle showed large differences between the steady and unsteady components of momentum addition. Calibration of the actuators provided a basic explanation of the observed airfoil per-

formance. For example, steady, relatively low momentum steady actuation was detrimental at $Re>100{,}000$, while beneficial at $Re=50{,}000$ due to the four-fold increase relative momentum addition.

Modulating the actuators at frequencies corresponding to $F^{+}\approx1$, resulted in improvements to $C_{L,\max}$, which increased with reductions in Re. At the low end of the MAV Reynolds number range ($Re=20{,}500$) modulation increased $C_{L,\max}$ by more than a factor of 2. In addition, hysteresis associated with the baseline airfoil was eliminated. Of particular interest from an applications perspective was that performance, measured here by $C_{L,\max}$, was shown to increase with decreasing duty cycle, and hence power input. In fact, duty cycles of around 3% were sufficient for effective separation control, corresponding to power inputs on the order of 500 milliwatts per unit length.

References

[1]   T.J. Mueller. "Aerodynamic Measurements at Low Reynolds Numbers for Fixed Wing Micro-Air Vehicles". Presented at the RTO AVT/VKI Special Course on Development and Operation of UAVs for Military and Civil Applications, VKI, Belgium, September 13-17, 1999.

[2]   T.J. Mueller (ed.). "Fixed and Flapping Wing Aerodynamics for Micro Air Vehicle Applications". In Progress in Aeronautics and Astronautics, Volume 195, 2001, pp. 115-142.

[3]   S.J. Morris. "Design and Flight Test Results for Micro-Signed Fixed-Wing and VTOL Aircraft". 1st International Conference on Emerging Technologies for Micro Air Vehicles, Georgia Institute of Technology, Atlanta Georgia, February 1997, pp. 117-131.

[4]   J.S. Attinello. "Design and Engineering Features of Flap Blowing Installations". In G.V. Lachmann. "Boundary Layer and Flow Control. Its Principles and Application", Volume 1, 1961, Pergamon Press, New York, pp. 463-515.

[5]   B.H. Carmichael. "Low Reynolds Number Airfoil Survey". NASA Contractor Report 165803, Volume I, November 1981.

[6]   J.R. Roth, D. Sherman and S. Wilkinson. "Boundary Layer Flow Control with One Atmosphere Uniform Glow Discharge Surface Plasma". AIAA 1998-0328, 1998.

[7]   D. Greenblatt and I. Wygnanski. "Control of separation by periodic excitation" In Progress in Aerospace Sciences, Volume 37, Issue 7, 2000, pp. 487-545.

[8] D. Greenblatt and I. Wygnanski. "Use of Periodic Excitation to Enhance Airfoil Performance at Low Reynolds Numbers". In AIAA Journal of Aircraft, Volume 38, Issue 1, 2001, pp. 190-192.

[9] B. Göksel. "Improvement of Aerodynamic Efficiency and Safety of Micro Aerial Vehicles by Separation Flow Control in Weakly Ionized Air". (in German) In Proceedings of the German Aerospace Congress, Leipzig, DGLR Paper JT-2000-203, 2000, pp. 1317-1331.

[10] B. Göksel and I. Rechenberg. "Active Separation Flow Control Experiments in Weakly Ionized Air". In Andersson H. I. and Krogstad P.-Å. (eds.) Advances in Turbulence X, Proceedings of the 10th Euromech European Turbulence Conference, CIMNE, Barcelona, 2004.

[11] T.C. Corke, C. He and M.P. Patel. "Plasma flaps and slats: An application of weakly ionized plasma actuators". AAIA Paper 2004-2127, 2nd AIAA Flow Control Conference, Portland, Oregon, 2004.

[12] C.L. Enloe, T.E. McLaughlin, R.D. Van Dyken, K.D. Kachner, E. J. Jumper and T.C. Corke. "Mechanism and Responses of a Single Dielectric Barrier Plasma Actuator: Plasma Morphology". In AIAA Journal, Volume 42, Issue 3, 2004, pp. 589-594.

[13] B. Göksel and I. Rechenberg. "Active Flow Control by Surface Smooth Plasma Actuators". In Rath H. J., Holze C., Heinemann H.-J., Henke, R. and Hönlinger H. (eds.) "New Results in Numerical and Experimental Fluid Mechanics V", Contributions to the 14th STAB/DGLR Symposium Bremen, Germany 2004, NNFM Vol. 92, Springer, 2006 (in press).

[14] B. Göksel and I. Rechenberg "Experiments to Plasma Assisted Flow Control on Flying Wing Models". Submitted for Proceedings of CEAS/KATnet Conference on Key Aerodynamic Technologies To Meet the Challenges of the European 2020 Vision, Bremen, 2005.

[15] B. Göksel, D. Greenblatt, I. Rechenberg and C. O. Paschereit "Plasma Actuators for Active Flow Control". DGLR Paper 2005-210, to be published in the Proceedings of the German Aerospace Congress 2006, Friedrichshafen, Germany, 2005.

[16] S. Margalit, D. Greenblatt, A. Seifert and I. Wygnanski "Delta wing stall and roll control using segmented piezoelectric fluidic actuators". In AIAA Journal of Aircraft, Volume 42, Issue 3, 2005, pp. 698-709.

[17] Ph. Poisson-Quinton and L. Lepage "Survey of French research on the control of boundary layer and circulation", in Lachmann, G. V., "Boundary layer and Flow Control. Its Principles and Application", Volume 1, Pergamon Press, New York, 1961, pp. 21-73.